

Niflumic Acid Alters Gating of HCN2 Pacemaker Channels by Interaction with the Outer Region of S4 Voltage Sensing Domains

Lan Cheng and Michael C. Sanguinetti

Nora Eccles Harrison Cardiovascular Research and Training Institute and Department of Physiology, University of Utah, Salt Lake City, Utah

Received December 23, 2008; accepted February 13, 2009

ABSTRACT

Niflumic acid, 2-[[3-(trifluoromethyl)phenyl]amino]pyridine-3-carboxylic acid (NFA), is a nonsteroidal anti-inflammatory drug that also blocks or modifies the gating of many ion channels. Here, we investigated the effects of NFA on hyperpolarization-activated cyclic nucleotide-gated cation (HCN) pacemaker channels expressed in *X. laevis* oocytes using site-directed mutagenesis and the two-electrode voltage-clamp technique. Extracellular NFA acted rapidly and caused a slowing of activation and deactivation and a hyperpolarizing shift in the voltage dependence of HCN2 channel activation (-24.5 ± 1.2 mV at 1 mM). Slowed channel gating and reduction of current magnitude was marked in oocytes treated with NFA, while clamped at 0 mV but minimal in oocytes clamped at -100 mV, indicating the drug preferentially interacts with chan-

nels in the closed state. NFA at 0.1 to 3 mM shifted the half-point for channel activation in a concentration-dependent manner, with an EC_{50} of 0.54 ± 0.068 mM and a predicted maximum shift of -38 mV. NFA at 1 mM also reduced maximum HCN2 conductance by $\sim 20\%$, presumably by direct block of the pore. The rapid onset and state-dependence of NFA-induced changes in channel gating suggests an interaction with the extracellular region of the S4 transmembrane helix, the primary voltage-sensing domain of HCN2. Neutralization (by mutation to Gln) of any three of the outer four basic charged residues in S4, but not single mutations, abrogated the NFA-induced shift in channel activation. We conclude that NFA alters HCN2 gating by interacting with the extracellular end of the S4 voltage sensor domains.

Niflumic acid (NFA) and other fenamates (e.g., flufenamic acid, mefenamic acid, meclofenamic acid) inhibit type 2 cyclooxygenase and are used as anti-inflammatory drugs to relieve acute pain and to treat rheumatoid arthritis. NFA has many other activities that are unrelated to its intended pharmacology. For example, NFA blocks or potentiates the effects of GABA on GABA_A receptors in a subunit-dependent manner (Sinkkonen et al., 2003), inhibits gap junction hemichannels (Eskandari et al., 2002), and affects the gating of many types of ion channels. NFA and other fenamates were first demonstrated to block Cl[−] channels (White and Aylwin, 1990; Scott-Ward et al., 2004), but these compounds also block Kv2.1 channels (Lee and Wang, 1999), activate large

conductance Ca²⁺-activated (Ottolia and Toro, 1994) and hERG1 (Malykhina et al., 2002) K⁺ channels, and alter the voltage dependence of gating of Kv4.2, Kv4.3 (Wang et al., 1997), KCNQ1/minK (Busch et al., 1994), KCNQ2/3 (Peretz et al., 2005), and HCN pacemaker (Accili and DiFrancesco, 1996; Satoh and Yamada, 2001) channels. For all channel types, the onset of NFA activity is very rapid, consistent with its binding to a site readily accessible from the extracellular side of the membrane. The three-dimensional structure of a complex formed between NFA and a receptor has only been determined for the enzyme phospholipase A2. In this case, NFA inhibits phospholipase A2 by interaction with the substrate binding site via the active-site residues His48 and Asp49 (Jabeen et al., 2005).

The effects of NFA on pacemaker current (i_f in heart or i_h in neurons) have been previously studied in cardiac myocytes (Accili and DiFrancesco, 1996) and in photoreceptors (Satoh and Yamada, 2001). Accili and DiFrancesco (1996) reported

This work was supported by the National Institutes of Health National Heart, Lung, and Blood Institute [Grant R01-HL65299].

Article, publication date, and citation information can be found at <http://molpharm.aspetjournals.org>.
doi:10.1124/mol.108.054437.

ABBREVIATIONS: NFA, niflumic acid (2-[[3-(trifluoromethyl)phenyl]amino]pyridine-3-carboxylic acid); WT, wild-type; G-V, conductance-voltage; HCN2, hyperpolarization-activated cyclic-nucleotide gated type 2; HCN2_{ntk}, N-terminal truncated HCN2; I-V, current-voltage; τ_f , fast time constant for current activation; τ_s , slow time constant for current activation; τ_{deact} , time constant for current deactivation; V_h , holding potential; V_t , test potential; $V_{1/2}$, half-point of activation curve; UL-FS49, zatebradine; ZD7288, 4-(N-ethyl-N-phenylamino)-1,2-dimethyl-6-(methylamino)-pyrimidinium chloride.

that NFA at 50 and 500 μM slows the pacing rate of rabbit sinoatrial node myocytes by slowing the kinetics of i_f and shifting its voltage dependence of activation to more negative potentials, without causing a change in slope conductance or ion selectivity. In newt rod photoreceptors, Satoh and Yamada (2001) reported that NFA at 100 μM slowed the activation and deactivation of i_h and reduced the steady-state current in a voltage-dependent manner, effects explained by a negative shift in the voltage dependence of channel activation. Similar to i_f in myocytes, the fully activated conductance of i_h in photoreceptors was not affected by 100 μM NFA. When applied to the bath solution, NFA did not affect pacemaker currents measured in excised inside-out patches of sinoatrial node myocytes (Accili and DiFrancesco, 1996) or rod photoreceptors (Satoh and Yamada, 2001), indicating that the drug binds to the extracellular side of the channel. Thus, NFA slows the rate of activation and decreases the amplitude of pacemaker current by affecting channel gating in native cells. However, the fenamate binding site has not been identified at the molecular level for pacemaker or any other type of ion channel.

Here, we characterize the mechanisms of action of NFA on cloned mammalian HCN2 channels heterologously expressed in *Xenopus laevis* oocytes. We test the hypothesis that NFA alters HCN2 channel gating by interacting with the basic residues located in the extracellular end of the S4 transmembrane domain, the main component of the voltage sensor.

Materials and Methods

Molecular Biology. mHCN2 cDNA was cloned from Marathon-Ready (Clontech, Mountain View, CA) mouse brain cDNA and inserted into the pSP64T oocyte expression vector as previously described (Chen et al., 2000). Mutations were introduced into N-terminal truncated mouse HCN2 (HCN2_{ntk}) cDNA as described previously (Chen et al., 2000). Restriction mapping and DNA sequencing of the polymerase chain reaction-amplified segment were used to confirm the presence of the desired mutation and the lack of extra mutations. cRNA for injection into oocytes was prepared with SP6 Capscribe (Roche, Indianapolis, IN) after linearization with EcoRI. RNA quality was checked by gel electrophoresis, and concen-

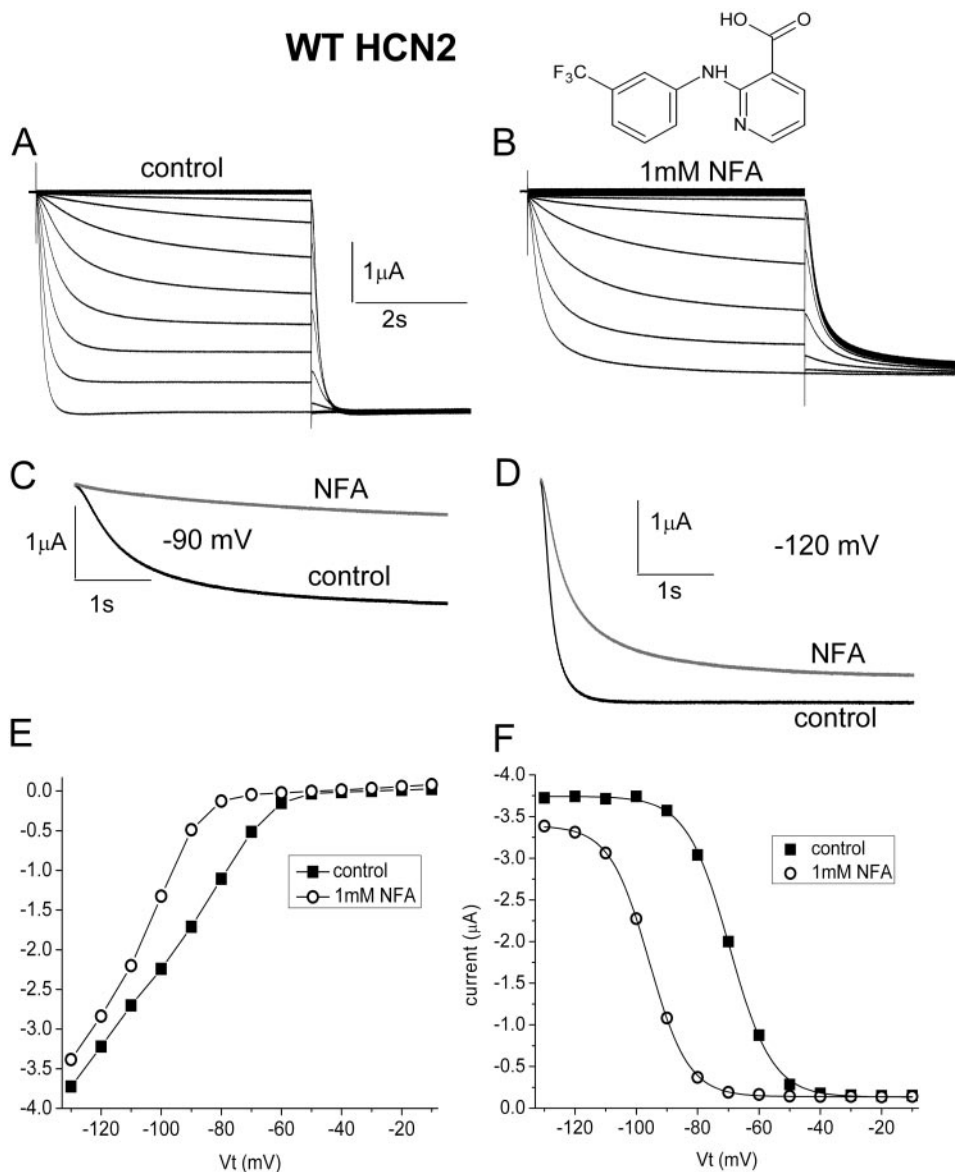


Fig. 1. NFA slows the rate of onset of WT HCN2 current activation and shifts its voltage dependence of activation to more negative potentials. A and B, WT HCN2 channel currents recorded from a single oocyte during 5-s pulses to test potentials ranging from -10 to -130 mV, applied in 10-mV steps. The V_h was -30 mV, recorded at a V_t of -90 mV (C) and -120 mV (D). Traces recorded before (control) and after exposure to 1 mM NFA are superimposed. At -90 mV, control: $\tau_f = 489$ ms, $\tau_s = 2400$ ms; $A_f/(A_f + A_s) = 0.64$; 1 mM NFA: $\tau_f = 3239$ ms. At -120 mV, control: $\tau_f = 140$ ms, $\tau_s = 448$ ms; $A_f/(A_f + A_s) = 0.96$; 1 mM NFA: $\tau_f = 258$ ms, $\tau_s = 1271$ ms; $A_f/(A_f + A_s) = 0.65$. E, I-V relationship measured before and after NFA. Currents were measured at the end of the 5-s pulse to the indicated V_t . F, effect of NFA on the voltage dependence of current activation. Currents were not corrected for instantaneous leak. Under control conditions the $V_{1/2}$ was -69 mV ($k = 7.1$ mV); after 1 mM NFA, $V_{1/2}$ was -96 mV and k was 6.5 mV. All data are from the same oocyte.

tration was quantified by UV spectroscopy and Ribogreen assay (Invitrogen, Carlsbad, CA).

Voltage Clamp of Oocytes. Isolation and maintenance of *X. laevis* oocytes and cRNA injections were performed as described previously (Goldin, 1991). In brief, stage IV and V *X. laevis* oocytes were injected with 10 to 50 ng of cRNA encoding WT or mutant HCN2_{ntk} channels. After injection with cRNA, the oocytes were cultured at 18°C for 1 to 3 days in Barth's solution containing 88 mM NaCl, 1 mM KCl, 1 mM MgSO₄, 0.41 mM CaCl₂, 2.4 mM NaHCO₃, 10 mM HEPES, 0.33 mM Ca(NO₃)₂, 50 µg/ml gentamycin, and 1 mM pyruvate, pH 7.4. For voltage-clamp experiments, oocytes were bathed in a modified ND96 external solution containing 96 mM NaCl, 4 mM KCl, 1 mM MgCl₂, 1 mM CaCl₂, and 5 mM HEPES, pH 7.6. Currents were recorded at room temperature (22–24°C) with a GeneClamp 500 amplifier (Molecular Devices, Sunnyvale, CA) using standard two-microelectrode voltage-clamp techniques (Stühmer, 1992). Current-voltage (I-V) relationships for WT and mutant channels were determined using 5-s test pulses applied from a holding potential (V_h) of –30 mV to test potentials (V_t) ranging from –130 to –30 mV. Pulses were applied once every 21 s. For all experiments, the oocyte recording chamber was constantly perfused with external solution at a rate of 2 ml/min. Drug-induced reduction of current was assessed by measuring inward current at the end of a 5-s hyperpolarizing pulse to –100 mV and calculating percentage reduction based on currents measured before drug and after complete block of HCN2 current with 20 mM CsCl.

To determine whether NFA preferentially affects HCN2 channels in the open or closed state, oocytes were treated with NFA, while the V_h was maintained at either 0 mV or –100 mV. At 0 mV, WT HCN2 channels are closed, whereas at –100 mV, most channels are in the open state. To assess drug interaction with closed channels, a single 2-s pulse to –100 mV (followed by a 1-s pulse to +20 mV to assess deactivation) was applied immediately before addition of NFA to assess current magnitude in the absence of drug. The oocyte was then clamped to 0 mV without pulsing while it was exposed to 1 mM NFA for 3 min. At the end of the 3-min incubation period, a single 2-s pulse to –100 mV was applied again and compared with the predrug current. To assess drug interaction with open channels, a 3-min pulse to –100 mV was applied from a V_h of 0 mV. After 30 s, the perfusate was switched from the modified ND96 + 1% DMSO (control) solution to one containing 1 mM NFA. The effect of NFA was assessed by comparing current magnitude at 30 s (predrug) versus current at 3 min (with drug).

The structure of NFA (2-([3-(trifluoromethyl)phenyl]amino)pyridine-3-carboxylic acid) is shown as an inset in Fig. 1B. NFA was purchased from Sigma-Aldrich (St. Louis, MO) and was prepared as a 100 mM stock solution in DMSO. An aliquot of this stock solution was dissolved in the modified ND96 external solution immediately before use to obtain the final desired drug concentrations. All solutions containing NFA were corrected to pH 7.6 with NaOH. The control solution always contained the same amount of DMSO as the NFA solution (e.g., 1% DMSO for 1 mM NFA).

Data Analysis. The fast and slow time constants for HCN2 current activation (τ_f , τ_s) at –100 mV were determined using the standard exponential curve fitting routine of pClamp 8 software (Molecular Devices). Time-dependent activating currents (I_{act}) were fitted with a two-exponential function: $I_{act}(t) = A_f e^{-t/\tau_f} + A_s e^{-t/\tau_s} + C$.

The time constants for deactivation (τ_{deact}) were determined at +20 mV after a test pulse to –130 mV. The effect of NFA on the voltage dependence of WT or HCN2_{ntk} channels was determined using 5-s pulses to a wide range of V_t . For WT channels, V_t ranged from –130 to –10 mV, but for some mutant channels, V_t was varied from –160 to –20 or –40 mV. Each V_t was followed by a second pulse to a potential of –130 mV (or –160 mV). The initial current amplitude recorded during the second pulse was corrected

for leak, defined as the instantaneous current after a prepulse to –10 mV. The leak-corrected currents were then plotted as a function of V_t , and the relationship was fitted with a Boltzmann function to determine the maximum current value (I_{max}) under control conditions. All current amplitudes from an individual oocyte were normalized to its own I_{max} , plotted as a function of V_t and fitted again with a Boltzmann function ($I/I_{max} = 1/[1 + \exp((V_t - V_{1/2})/k)]$) using Origin 7.5 software (OriginLab Corp., Northampton, MA) to determine the values of the half-point ($V_{1/2}$) and the slope factor (k) for channel activation.

The shift in $V_{1/2}$ ($\Delta V_{1/2}$, in mV) was plotted as a function of [NFA], and the data were fit to a dose-response logistic function ($\Delta V_{1/2} = V_{max} + V_{max}/[1 + ([NFA]/EC_{50})^{n_H}]$) using Origin 7.5, where V_{max} is the maximal shift in $V_{1/2}$, EC_{50} is the drug concentration required for 50% of the maximum shift in $V_{1/2}$, and n_H is the Hill coefficient.

Data are presented as mean \pm S.E. (n = number of oocytes), and statistical comparisons between experimental groups were per-

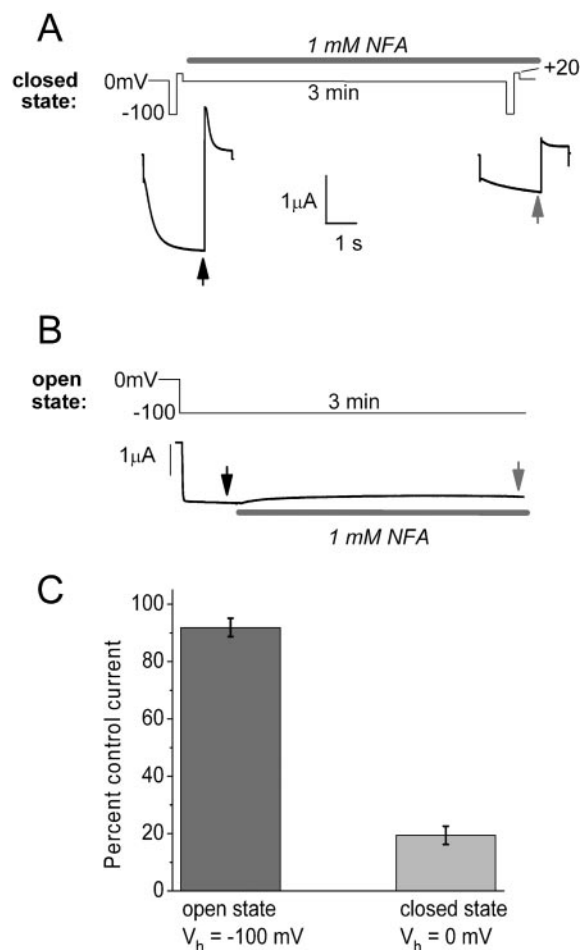


Fig. 2. State-dependent modification of WT HCN2 channels by NFA. A, test for effects of NFA on closed channels. Top, voltage pulse protocol and timing of NFA exposure. A test pulse was applied before NFA, and once again after 3 min application of 1 mM NFA. The V_h was 0 mV between test pulses. Lower panel shows the two test currents on an expanded time scale. Current activation was elicited with a 2-s pulse to –100 mV followed by a 1-s pulse to +20 mV to induce deactivation. Current magnitude was defined as time-dependent inward current measured at the end of pulse (indicated by arrows) minus the instantaneous current at start of pulse. B, test for effects of NFA on open channels. Top, voltage pulse protocol. Bottom, inward current at a V_h of –100 mV, the times where current magnitude was measured (indicated by arrows) and the timing of NFA exposure. C, reduction of HCN2 current by NFA, defined as percentage of time-dependent current measured at –100 mV after 3 min of drug compared with current measured before drug exposure.

formed using two-way ANOVA and the Student's *t* test. Differences were considered significant at $p < 0.05$.

Results

NFA Reduces the Amplitude and Slows Kinetics of HCN2 Channel Currents. We first determined the effects of 1 mM NFA on currents conducted by WT HCN2 channels expressed in *X. laevis* oocytes. Currents were elicited with 5-s pulses applied to V_t ranging from -10 to -130 mV. After each test pulse, the membrane potential was pulsed to -130 mV for 3 s (Fig. 1A). NFA slowed the rate of current activation and reduced current amplitude at all test potentials (Fig. 1B), but the reduction was more pronounced at -90 mV (Fig. 1C) than at -120 mV (Fig. 1D). The voltage dependent suppression of current by NFA is readily apparent in the I-V plot (Fig. 1E) and was caused by both a reduction in maximum conductance and a shift of the voltage dependence of activation to more negative potentials (Fig. 1F).

Similar results were obtained in seven oocytes, where the $V_{1/2}$ for activation was shifted by an average of -30.4 mV by 1 mM NFA.

As described under *Materials and Methods*, two pulse protocols were used to determine whether the effects of NFA on WT HCN2 channels were state-dependent. Modification of channels in the closed state was assessed by treating oocytes with 1 mM NFA while maintaining V_h at 0 mV. Test currents were elicited with a 2-s pulse applied to -100 mV immediately before and after 3-min incubation with NFA (Fig. 2A). Interaction of drug with open channels was assessed by switching the perfusate from a drug-free solution to one containing 1 mM NFA 30 s after the start of a 3-min pulse to -100 mV (Fig. 2B). The experiments were performed on five oocytes for each pulse protocol and are summarized as a bar plot in Fig. 2C. When channels were maintained in a closed state during treatment with NFA, the current elicited by the second test pulse activated and deactivated slower, and was reduced to $19 \pm 3\%$ of the peak inward current measured

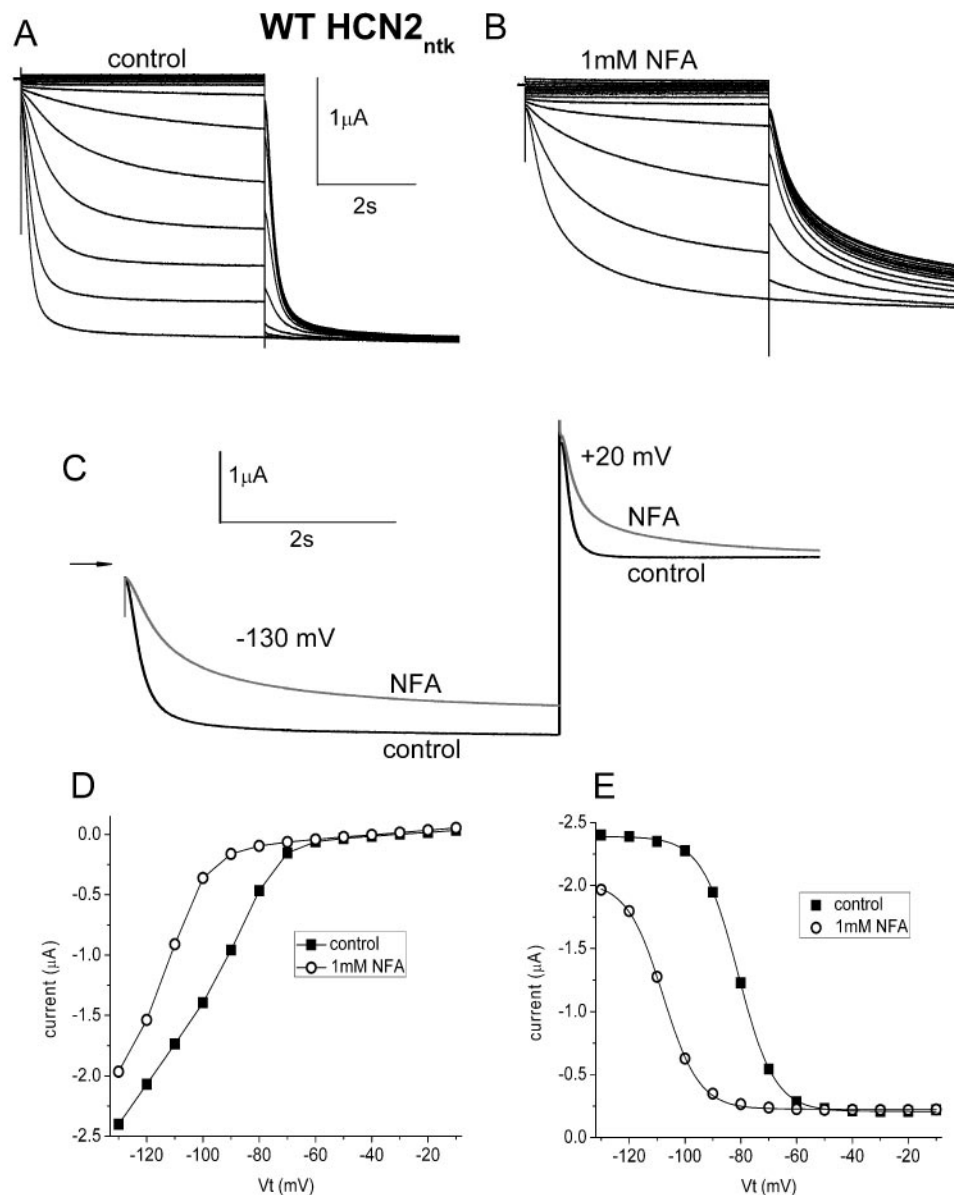


Fig. 3. NFA slows the activation rate and shifts the voltage dependence of activation of WT HCN2_{ntk} channel currents to more negative potentials. A and B, WT HCN2_{ntk} channel currents recorded from a single oocyte during 5-s pulses to test potentials ranging from -10 to -130 mV, applied in 10-mV steps, before (A) and after application of 1 mM NFA (B). The V_h was -30 mV and a pulse to -130 mV was applied after each test pulse. C, NFA slowed the rate of activation and deactivation of HCN_{ntk} channel current. For control: $\tau_f = 159$ ms, $\tau_s = 1315$ ms; $A_f/(A_f + A_s) = 0.87$. $\tau_{deact} = 80$ ms, 162 ms, $A_f/(A_f + A_s) = 0.84$. For 1 mM NFA: $\tau_f = 366$ ms, $\tau_s = 1944$ ms; $A_f/(A_f + A_s) = 0.60$. $\tau_{deact} = 145$ ms, 1110 ms, $A_f/(A_f + A_s) = 0.62$. D, I-V relationship measured before and after NFA. Currents were measured at the end of the 5-s pulse to the indicated V_t . E, voltage dependence of current activation. Control: $V_{1/2} = -81$ mV, $k = 6.48$ mV; 1 mM NFA: $V_{1/2} = -108$ mV; $k = 6.58$ mV. All data are from the same oocyte.

during the first pulse. This marked reduction and slowed gating is the expected consequence of the negative shift in the voltage dependence of activation measured at steady-state conditions (Fig. 1). In contrast, when channels were maintained in an open state during exposure to NFA, current was only slightly reduced ($92 \pm 3\%$ of control value). Thus, NFA preferentially affects channels in the closed state. The rapid onset and small reduction in current magnitude observed with the open state pulse protocol suggests that this reduction represents open channel block. In contrast, the large reduction in current and slowed activation induced by NFA when the V_h was maintained at 0 mV indicates that the drug preferentially interacts with channels in the closed state to induce the negative shift in the voltage dependence of HCN2 activation.

We next determined the effect of 1 mM NFA on the voltage dependence of N-truncated HCN2 (HCN2_{ntk}) channels. This construct was used because several mutant forms of this altered channel have been previously characterized (Chen et al., 2000) and these mutants are used later in this study. HCN2_{ntk} channel current was activated at more negative potentials than WT HCN2 but the effect of NFA was similar, causing a slowing of activation and a reduction of current measured at the end of the 5-s pulse (Fig. 3, A–C). In addition, NFA slowed the rate of current deactivation measured at +20 mV after a test pulse to –130 mV (Fig. 3C). Also similar to WT HCN2, 1 mM NFA caused a leftward shift of the I–V relationship (Fig. 3D) and the voltage dependence of current activation (Fig. 3E) for HCN2_{ntk} channels. The aver-

aged and normalized I–V relationship determined for multiple oocytes ($n = 16$) is plotted in Fig. 4A. The voltage dependence of current activation, normalized to I_{\max} for each oocyte is plotted in Fig. 4B. The average $V_{1/2}$ of WT HCN_{ntk} channels under control conditions was -77.6 ± 0.9 mV. In the presence of 1 mM NFA, the $V_{1/2}$ was -102.0 ± 1.2 , an average shift of -24.5 ± 1.2 ($n = 16$). The slope factor (k) for the relationship (7.5 ± 0.2 mV) was not significantly altered by NFA ($k = 7.7 \pm 0.2$ mV). Extrapolation of the curves from the Boltzmann fits to more negative potentials was used to estimate that 1 mM NFA reduced the maximum conductance of HCN2_{ntk} channel current by 22%. This reduction in current amplitude was in addition to that caused by the leftward shift in the voltage dependence of current activation. The reduction in current amplitude could be related to changes in channel gating; however, a similar reduction in current was also observed for Y331D HCN2 channels that are constitutively open and do not exhibit any time-dependent gating (Chen et al., 2001). Current recorded at –100 mV for this mutant channel was reduced by $28 \pm 2\%$ ($n = 8$, not shown). Thus, the reduction in current induced by 1 mM NFA is probably caused by occlusion of the pore and results from drug binding to a receptor site distinct from the site that mediates altered channel gating.

The effect of NFA on the voltage dependence of HCN2_{ntk} channel activation was concentration-dependent. The shift in $V_{1/2}$ for activation was determined at four concentrations, ranging from 0.1 to 3 mM (Fig. 4C). The EC_{50} for this effect was $542 \pm 68 \mu\text{M}$ ($n_H = 0.97$). The maximum NFA-induced

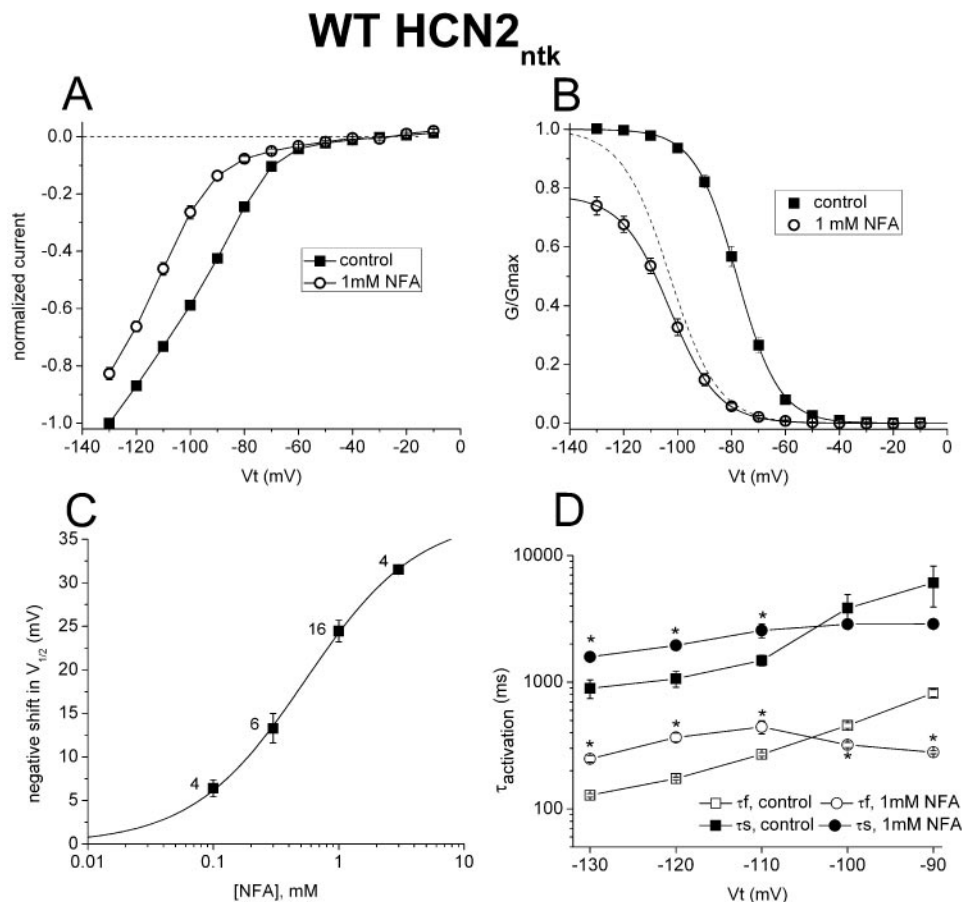


Fig. 4. NFA causes concentration-dependent shift in the voltage dependence of WT HCN_{ntk} channel activation. **A**, normalized I–V relationships recorded before and after treatment of oocytes to 1 mM NFA ($n = 16$). For most data points, the small S.E. bars are masked by the larger symbols. **B**, effect of 1 mM NFA on normalized voltage dependence of current activation (G – V relationship). The $V_{1/2}$ of WT HCN_{ntk} channels was -77.6 ± 0.9 mV and slope factor, k was 7.5 ± 0.2 mV; after treatment with 1 mM NFA, $V_{1/2}$ was -102.0 ± 1.2 mV and k was 7.7 ± 0.2 mV ($n = 16$). The dotted curve represents NFA data normalized to its own peak value. **C**, [NFA]-dependent shift in voltage dependence of HCN2_{ntk} channel activation. The EC_{50} for the NFA-induced shift in $V_{1/2}$ was $542 \pm 68 \mu\text{M}$ ($n_H = 0.97$). The maximum shift in $V_{1/2}$ predicted by extrapolation of the Hill plot was -38 mV. **D**, kinetics of activation. Plotted data represent the average fast (open symbols) and slow (filled symbols) time constants for the onset of current activation during 5-s pulses at the indicated V_t . * $p < 0.01$ compared with matched control.

shift in $V_{1/2}$ predicted by extrapolation of the Hill plot was -38 mV. NFA slowed the rate of current activation, measured as fast and slow time constants, at a V_t of -110 to -130 mV but decreased the fast time constant for activation at -90 mV (Fig. 4D).

Neutralization of Single Basic Residues in Outer S4 Domain Does Not Prevent NFA-Induced Shift in Activation of HCN_{2ntk} Channels. The S4 domain of HCN2 channels has nine basic residues (Fig. 5A), and it has been proposed (Chen et al., 2000) that the four outermost (N-terminal) basic residues are located outside the membrane when the channel is either in a closed or open state. Neutralization of one or more of these charged residues causes a graded shift in the voltage dependence of activation to more negative potentials (Chen et al., 2000; Vaca et al., 2000), similar to the effect of NFA. We hypothesized that perhaps the acidic group of NFA might interact with one or more of these basic residues to mimic charge neutralization and hence, also cause channels to activate at more negative potentials. Therefore, we neutralized each of these residues (Lys291, Arg294, Arg297, or Arg300) by mutating it to a Gln

and determined whether this altered the response of the mutant channel to 1 mM NFA. In addition, Lys291 was also mutated to a Glu, causing a reversal in charge at this position in the S4 domain. As previously reported, the mutations altered the $V_{1/2}$ and slope factor of the activation curves, but none of the single mutations prevented the negative shift in the voltage dependence of activation caused by NFA (Fig. 5, Table 1). A notable exception was the K291Q mutation. NFA shifted the $V_{1/2}$ for K291Q HCN_{2ntk} channels the least, by only -15.3 ± 1.0 mV ($n = 4$). This difference is of doubtful significance because charge reversal at this position (K291E) responded to NFA in the usual manner with a shift in $V_{1/2}$ of -24.3 ± 1.7 mV ($n = 5$). In addition, NFA reduced the magnitude of whole cell current by ~ 20 to 30% in oocytes expressing any of the channels harboring a single S4 mutation as estimated by extrapolation of the Boltzmann fitted curves to more negative potentials (Fig. 5). However, unlike WT HCN2 or HCN_{2ntk} channels, NFA caused only minor effects on the kinetics of current activation over the range of potentials examined (Fig. 6).

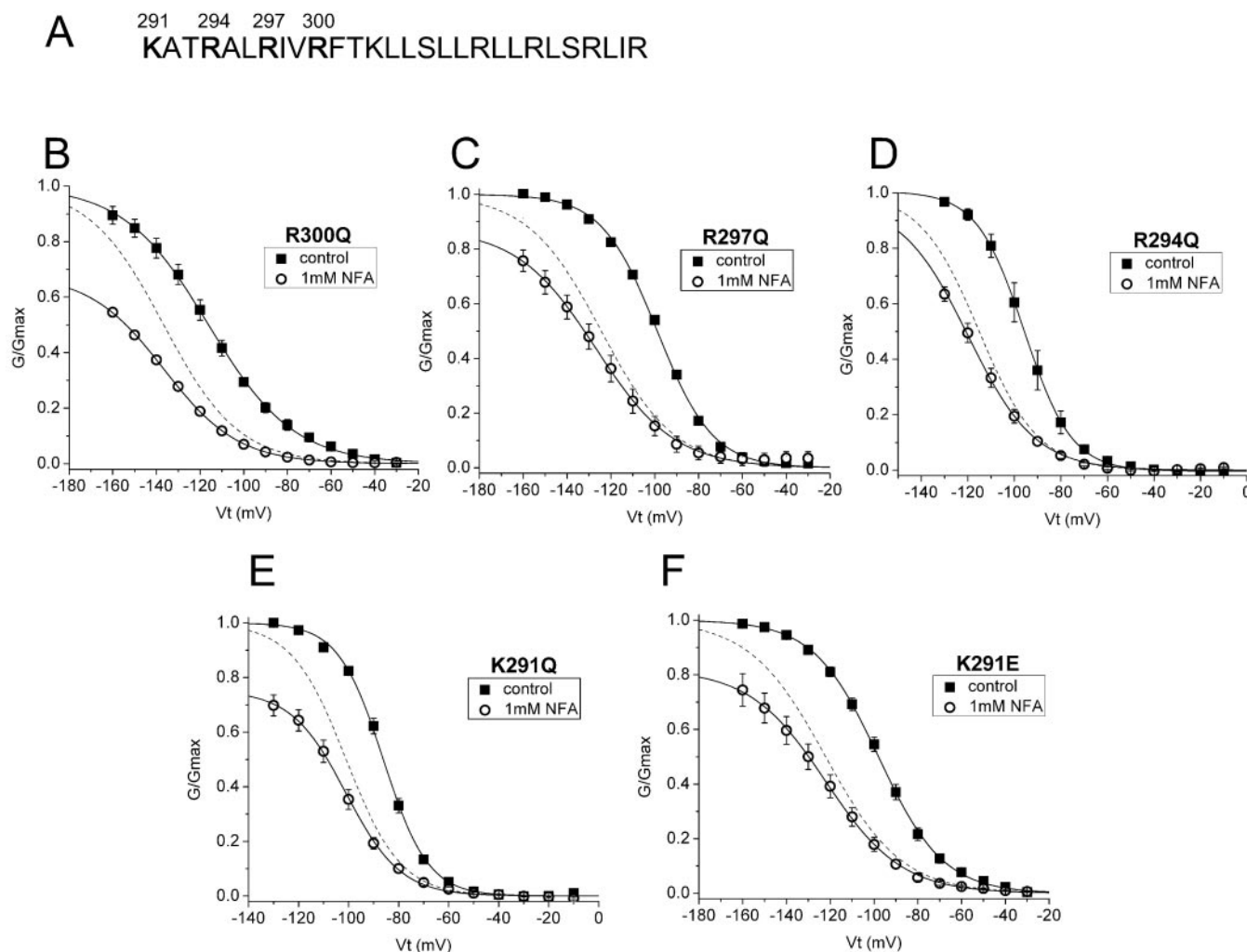


Fig. 5. Neutralization of single basic residues in S4 domain does not prevent NFA-induced negative shift in the voltage dependence of activation of HCN_{2ntk} channels. A, sequence of the HCN2 S4 domain. B to F, normalized I-V relationships recorded before and after treatment of oocytes to 1 mM NFA. The single mutation introduced into the Arg or Lys residue in the S4 domain is indicated for each channel type. Smooth curves represent Boltzmann fit to the data. The dotted curves represent NFA data normalized to its own peak value. The values for $V_{1/2}$ and k for the Boltzmann function are listed in Table 1.

TABLE 1
Effects of 1 mM NFA on voltage dependence of activation and kinetics of deactivation of WT and mutant HCN2_{ntk} channels

Channel	Pulse Duration s	V _{1/2}		ΔV _{1/2}		k		n		τ _{deact} + 20 mV	
		Control	NFA	mV	mV	Control	NFA	Control	NFA	Control	NFA
WT HCN2	5	-72.5 ± 1.7	-103.0 ± 1.4*	-30.4 ± 1.4	7.2 ± 0.4	7	6.9 ± 0.2	128 ± 7	684 ± 111*	ms	
WT HCN2 _{ntk}	5	-77.6 ± 0.9	-102.0 ± 1.2*	-24.5 ± 1.2	7.5 ± 0.2	16	7.7 ± 0.2	154 ± 8	230 ± 8*		7
K291E HCN2 _{ntk}	5	-97.9 ± 1.7	-122.2 ± 1.3*	-24.3 ± 1.7	14.7 ± 0.3	5	17.1 ± 0.5	86 ± 7	119 ± 3*		5
K291Q HCN2 _{ntk}	5	-85.1 ± 1.4	-103.5 ± 1.7*	-15.3 ± 1.0	8.8 ± 0.1	4	11.2 ± 0.8	177 ± 3	251 ± 14*		6
R294Q HCN2 _{ntk}	5	-95.1 ± 2.4	-115.7 ± 2.5*	-19.9 ± 1.6	9.1 ± 0.4	6	12.5 ± 0.4	102 ± 7	124 ± 6*		7
R297Q HCN2 _{ntk}	5	-100.9 ± 0.8	-126.9 ± 1.7*	-26.1 ± 2.0	12.2 ± 0.5	7	14.5 ± 1.0	245 ± 12	286 ± 28		6
R300Q HCN2 _{ntk}	5	-116.5 ± 2.7	-137.3 ± 2.4*	-20.9 ± 1.7	19.5 ± 1.7	5	17.2 ± 0.6	322 ± 10	318 ± 16		6
K291Q/R294Q/R297Q/R300Q HCN2 _{ntk}	5	-136.0 ± 0.7	-129.1 ± 1.7*	+6.8 ± 1.3 [†]	18.1 ± 2.0	9	14.3 ± 0.8	218 ± 27	263 ± 9		4
K291Q/R294Q/R297Q HCN2 _{ntk}	1	-129.4 ± 2.6	-123.0 ± 2.5*	+6.4 ± 1.0 [†]	13.5 ± 0.5	4	13.0 ± 0.8	141 ± 12	180 ± 3*		4
R294Q/R297Q/R300Q HCN2 _{ntk}	1	-114.7 ± 2.6	-116.8 ± 3.2	-2.1 ± 1.1 [†]	16.1 ± 1.3	6	14.9 ± 0.5	246 ± 9	251 ± 12		4
K291Q/R294Q/R300Q HCN2 _{ntk}	5	-132.8 ± 0.3	-131.2 ± 1.2	+1.6 ± 1.0 [†]	17.0 ± 0.3	3	17.9 ± 0.7	73 ± 4	134 ± 7*		4
K291Q/R297Q/R300Q HCN2 _{ntk}	1	-130.0 ± 4.8	-129.1 ± 2.7	+0.8 ± 2.7 [†]	14.4 ± 0.6	7	10.9 ± 0.8				
K291Q/R297Q/R300Q HCN2 _{ntk}	5	-136.5 ± 1.5	-133.3 ± 2.3	+3.1 ± 1.3 [†]	16.0 ± 0.8	3	14.7 ± 0.9				
K291Q/R297Q/R300Q HCN2 _{ntk}	5	-130.5 ± 2.1	-126.6 ± 4.3	+3.9 ± 2.2 [†]	18.3 ± 0.3	3	15.2 ± 0.6				
K291Q/R297Q/R300Q HCN2 _{ntk}	5	-129.9 ± 1.3	-121.3 ± 1.4*	+8.6 ± 0.9 [†]	10.1 ± 0.4	6	7.7 ± 0.1				

*p > 0.01 compared with matched control.
†p > 0.01 compared with WT HCN2_{ntk}.

Neutralization of Multiple Basic Residues in Outer S4 Domain Prevents NFA-Induced Shift in Activation of HCN_{ntk} Channels. We next determined the effects of NFA on HCN2_{ntk} channels with all four of the outermost basic residues neutralized by mutation to Gln (K291Q/R294Q/R297Q/R300Q). As reported previously (Chen et al., 2000), this “quadruple” mutant channel activated more rapidly and at more negative potentials than WT HCN2 channels. In contrast to WT HCN2 channels, 1 mM NFA only slightly slowed the kinetics of activation or deactivation of the quadruple mutant channel (Fig. 7, A and B). The voltage dependence of current activation was determined in two groups of oocytes. In the first group (n = 4), currents were activated with 1-s test pulses. NFA at 1 mM caused a slight rightward shift (+6.4 ± 1.0 mV) in the voltage dependence of activation and a reduction in maximum conductance of 14% (Fig. 7C). A second group of oocytes (n = 9) was activated using the usual 5-s test pulses and a similar rightward shift in V_{1/2} (+6.8 ± 1.3 mV) was observed, along with a reduction in maximal conductance of 18% (Fig. 7D). Thus, unlike WT channels or those harboring a single S4 mutation, neutralization of all four of the outer basic residues in the S4 domain induced a positive shift in the voltage dependence of activation.

Because single mutations did not prevent the negative shift in activation induced by NFA, whereas the quadruple mutant caused a slight shift in the opposite direction, we reasoned that NFA requires interaction with more than one basic residue in the outer region of S4 to exert its effect on channel gating. To explore this possibility, mutant channels containing neutralization of three of the four basic residues were constructed. Four different mutant channels were prepared and characterized: Lys291/Arg294/Arg297 (Fig. 8), Arg294/Arg297/Arg300 (Fig. 9), Lys291/Arg294/Arg300, and Lys291/Arg297/Arg300 (not shown). Similar to the quadruple mutant channel, these triple mutant channels were also relatively insensitive to NFA-induced changes in gating, but a reduction in current amplitude, presumably caused by channel block, was still observed. Lys291/Arg294/Arg300 and Lys291/Arg297/Arg300 HCN2_{ntk} channel activation was shifted to more positive potentials by NFA. A summary of the NFA-induced shifts in V_{1/2} for activation of WT and mutant HCN2_{ntk} channels is provided in Fig. 10.

Discussion

Fenamates possess a complicated pharmacology, affecting a number of enzymes and ion channels. NFA in particular has been subjected to intense scrutiny and either blocks and/or activates seemingly any channel chosen for investigation. Despite the amount of attention devoted to the mechanisms of action of NFA and other fenamates, the molecular basis of NFA binding to ion channels remains a mystery. The most thorough mechanistic studies have been performed by Camerino and colleagues (Liantonio et al., 2006, 2008; Picollo et al., 2007) and concern the modulation of ClC-K Cl⁻ channels by NFA and other fenamates. NFA binds to two different receptor sites on ClC-Ka channels. At low concentrations (50–500 μM), NFA is an activator, but higher concentrations (1–2 mM) block these channels (Liantonio et al., 2006). In contrast, other fenamates such as flufenamic acid only block ClC-Ka currents. Modeling predicts that when only one site

is occupied, NFA increases ClC-Ka currents, whereas the occupation of both binding sites leads to channel block (Piccolo et al., 2007). Evaluation of the sensitivity of ClC-Ka to derivatives of NFA and flufenamic acid suggests that the major feature of activating compounds is the coplanarity of the two rings of the molecules, whereas block is favored when the fenamate assumes a noncoplanar configuration (Liantonio et al., 2006; Liantonio et al., 2008). It is likely that NFA also binds to two distinct receptors on HCN2 channels – one resulting in a shift in the voltage dependence of gating, the other causing channel block.

For all channels types that have been investigated, the onset of block or altered gating induced by NFA is very rapid, consistent with its binding to a site readily accessible from the extracellular side of the membrane. However, a specific binding site for NFA or other fenamates has not been identified for any channel. We recently reported that 1 mM NFA shifts the half-point for activation of ERG1 and ERG2 channels by -6 and -18 mV, respectively. This channel subtype-specific activity was explored with chimeric channels and site-directed mutagenesis. The sensitivity of ERG1 channels to NFA could be increased to match ERG2 by swapping of their S3-S4 linker domains, equivalent to a point mutation (Gly to Arg) plus the addition of three Thr residues into ERG1. However, we did not identify mutations that could eliminate the sensitivity of ERG channels to NFA. In the

present study, we found that the effects of NFA on HCN2 channels could be abrogated by mutation of multiple charged residues located in the extracellular region of S4.

Despite a similar overall molecular topology, the voltage dependence of HCN channel gating is opposite to that of Kv channels. HCN channels are closed at depolarized potentials and open in response to hyperpolarization of the membrane. Activation of the sea urchin sperm pacemaker channel is associated with inward gating currents (Männikkö et al., 2002), consistent with an inward movement of the putative voltage sensing S4 domain that was confirmed by substituted cysteine accessibility mutagenesis experiments in sea urchin sperm pacemaker and MVP, an archaeobacterial HCN-like channel (Sesti et al., 2003). Each S4 domain of an HCN channel has nine basic residues (Arg or Lys) and a single Ser residue that are located in every third position of the α -helix. The Ser residue is located near the middle of S4, separating the charged amino acids into an outer (N-terminal) group of five, and an inner (C-terminal) group of four basic residues (Fig. 5A). In HCN1 channels, substituted cysteine accessibility mutagenesis analysis revealed that all five basic residues in the outer group were accessible to the Cys-modifying reagent MTSET regardless of membrane potential (Bell et al., 2004; Vemana et al., 2004). Only residues located in the inner group changed accessibility with a change in voltage. In addition, neutralization of each of the four outer charged

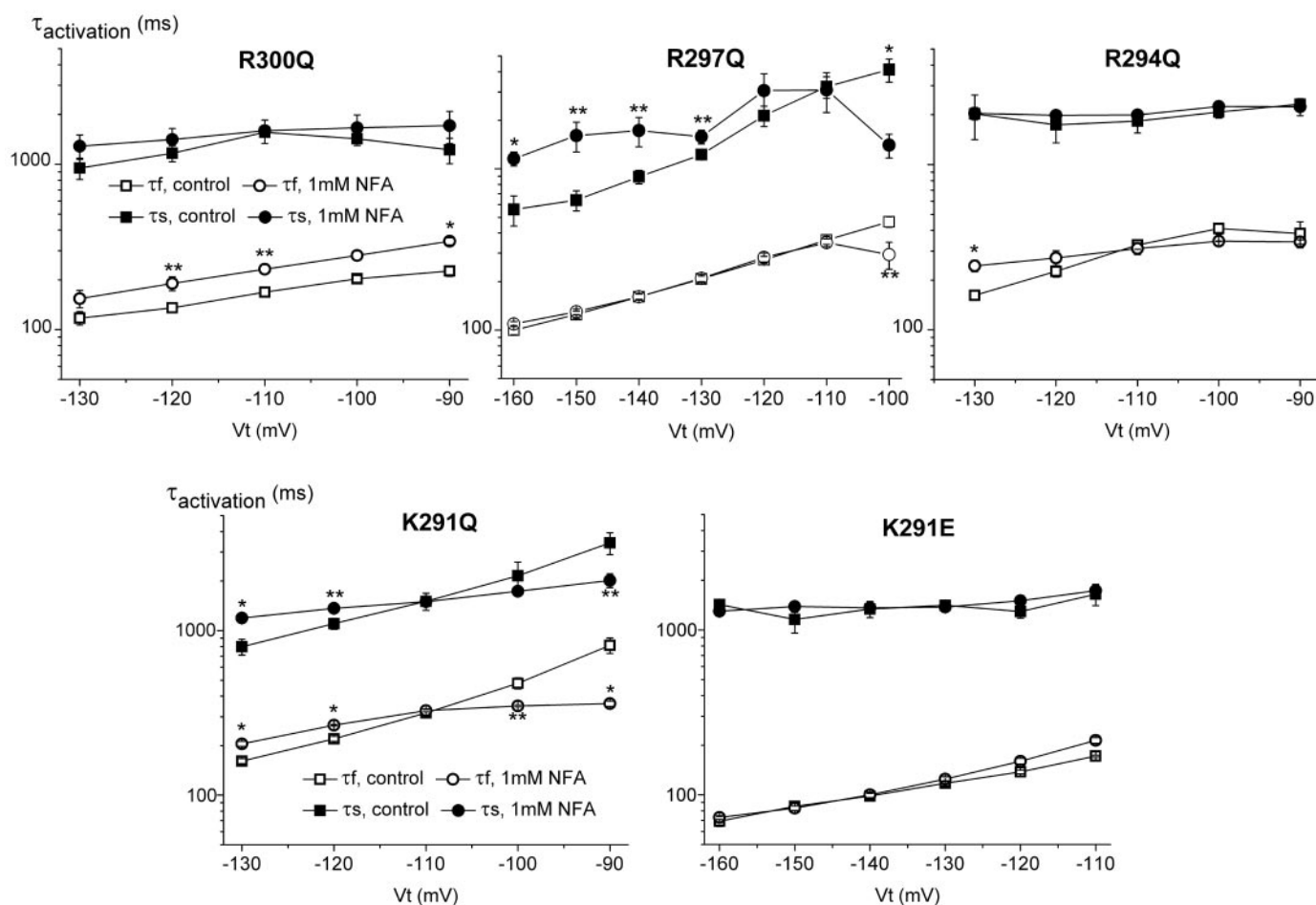


Fig. 6. Effect of 1 mM NFA on activation kinetics of HCN2_{ntk} channels containing a single S4 mutation. The S4 residue mutation is indicated at the top of each graph. Plotted data represent the average fast (open symbols) and slow (filled symbols) time constants for the onset of current activation during 5-s pulses at the indicated V_t . * $p < 0.01$; ** $p < 0.05$ compared with matched control.

K291Q/R294Q/R297Q/R300Q

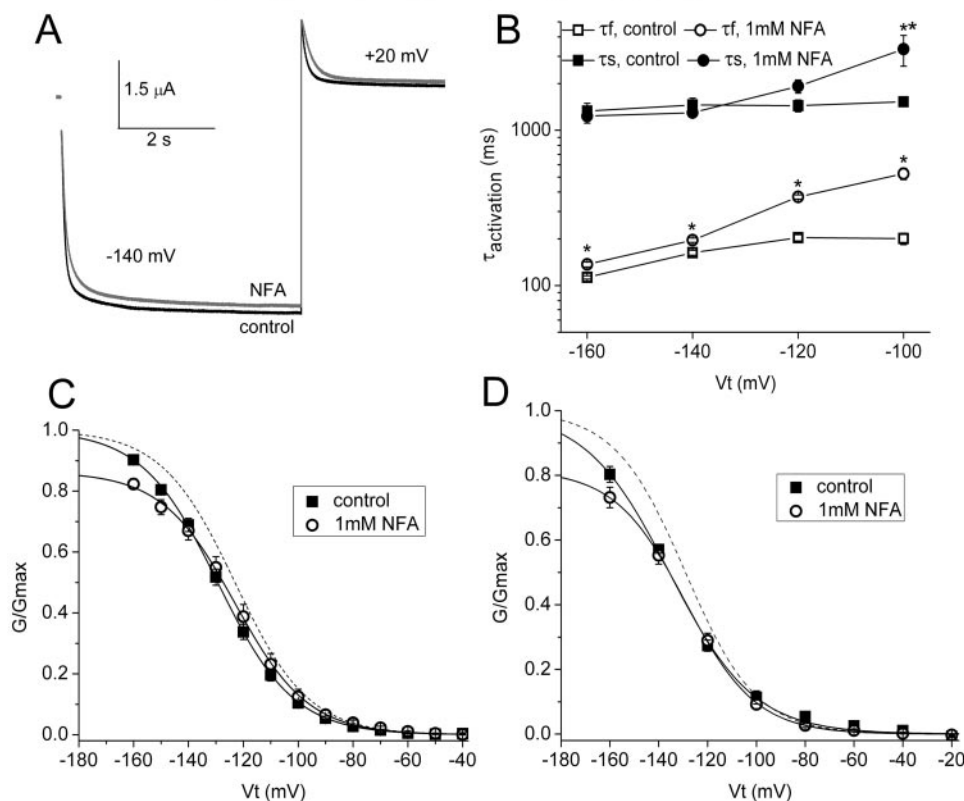


Fig. 7. Neutralization of four outer basic residues in S4 domain abolishes NFA-induced negative shift in HCN2_{ntk} channel activation. A, quadruple mutant channel currents recorded from an oocyte during 5-s activating pulses to a test potentials of -140 mV, followed by pulse to $+20$ mV to record channel deactivation. For control: $\tau_f = 67$ ms, $\tau_s = 1017$ ms; $A_f/(A_f + A_s) = 0.83$. $\tau_{\text{deact}} = 154$ ms. For 1 mM NFA: $\tau_f = 98$ ms, $\tau_s = 1008$ ms; $A_f/(A_f + A_s) = 0.81$. $\tau_{\text{deact}} = 194$ ms. B, effect of 1 mM NFA on the kinetics of activation. Plotted data represent the average fast (open symbols) and slow (filled symbols) time constants for the onset of current activation during 5-s pulses at the indicated V_t . $*$, $p < 0.01$; $**$, $p < 0.05$ compared with matched control. C and D, normalized G-V relationships recorded before and after treatment of oocytes to 1 mM NFA. The test pulse durations used to elicit current were either 1 s (C) or 5 s (D). Smooth curves represent Boltzmann fit to the data. The dotted curves represent NFA data normalized to its own peak value. The values for $V_{1/2}$ and k for the Boltzmann function are listed in Table 1.

K291Q/R294Q/R297Q

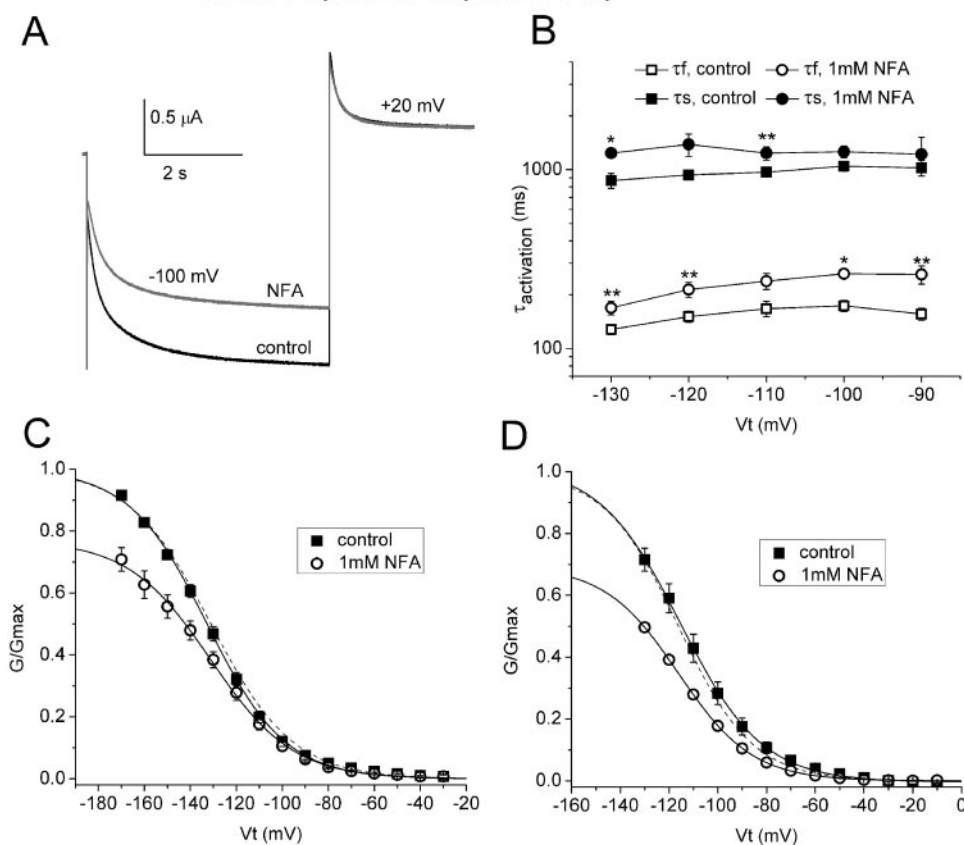


Fig. 8. Neutralization of three basic residues in S4 domain prevents NFA-induced negative shift in the voltage dependence of activation of HCN2_{ntk} channels. A, triple mutant (K291Q/R294Q/R297Q) channel currents recorded from an oocyte during 5-s activating pulse to -100 mV, followed by pulse to $+20$ mV to record channel deactivation. For control: $\tau_f = 179$ ms, $\tau_s = 1539$ ms; $A_f/(A_f + A_s) = 0.56$. $\tau_{\text{deact}} = 162$ ms. For 1 mM NFA: $\tau_f = 228$ ms, $\tau_s = 1497$ ms; $A_f/(A_f + A_s) = 0.61$. $\tau_{\text{deact}} = 217$ ms. B, effect of 1 mM NFA on the kinetics of activation. Plotted data represent the average fast (open symbols) and slow (filled symbols) time constants for the onset of current activation during 5-s pulses at the indicated V_t . $*$, $p < 0.01$; $**$, $p < 0.05$ compared with matched control. C and D, normalized G-V relationships recorded before and after treatment of oocytes to 1 mM NFA. The test pulse durations used to elicit current were either 1 s (C) or 5 s (D). Smooth curves represent Boltzmann fit to the data. The dotted curves represent NFA data normalized to its own peak value.

residues in HCN2 causes a cumulative hyperpolarizing shift in the voltage dependence of activation (Chen et al., 2000; Vaca et al., 2000). Interestingly, mutation of the four basic residues in the outer half of S4 have only minor effects on the kinetics of current activation (Vaca et al., 2000). Neutralization of all four charges caused a shift that was equal to the sum of the individual shifts (Vaca et al., 2000), suggesting that the outer charged residues screen negative surface charge (Chen et al., 2000) and allow the channel to open at more physiological voltages (Männikkö et al., 2002). Taken together, these studies suggest that compared with Kv channels, the S4 domain in HCN channels may undergo a minor translocation in response to changes in transmembrane voltage (Bell et al., 2004; Vemana et al., 2004), and that the outer four charged residues of S4 are always accessible from the extracellular space. Similar to the effects of neutralizing some of the positively charged residues in S4, NFA shifts the voltage dependence of HCN2 activation to more negative potentials. NFA exerts this effect from the extracellular side of the membrane, leading to our hypothesis that the acidic drug might shift activation by interaction with one or more basic charge in the outer S4. Although neutralization of the single outermost Lys or any one of the next three Arg failed to blunt the gating effects of NFA, we found that combined mutations prevented the negative shift in $V_{1/2}$ for activation. In addition, for some of the triple mutant channels, NFA caused a slight positive shift in $V_{1/2}$. Finally, HCN2 channels were modified in a state-dependent manner. Drug effects were marked when the oocyte was clamped to 0 mV, but minimal when clamped to -100 mV, indicating that NFA requires interaction with channels in the closed state to exert

its effects on gating. This finding is consistent with the idea that the extracellular binding site for NFA that mediates altered gating is inaccessible at negative membrane potentials because the S4 is retracted inward. However, although membrane hyperpolarization induces an inward movement of the S4 voltage sensor in sperm HCN channels as assessed by intramembrane charge displacement (Männikkö et al., 2002), membrane hyperpolarization does not alter the methanethiosulfonate ethyltrimethylammonium accessibility of the outer four basic residues in the S4 domain of HCN1 channels (Bell et al., 2004). An alternative mechanism to explain the state-dependent effects of NFA is that outer region of the S4 domain undergoes a voltage-dependent rearrangement in response to hyperpolarization that disfavors the binding of NFA but does not alter interaction of methanethiosulfonate ethyltrimethylammonium with a single introduced Cys residue. The small decrease in current magnitude that was observed when NFA was applied to cells held at -100 mV is consistent with open channel block, presumably mediated by drug binding to the outer region of the pore. In summary, our findings suggest, but do not prove, that NFA directly interacts with outer S4 residues in HCN2. Radiolabeled binding studies could possibly resolve this issue; however, the very low potency of NFA ($EC_{50} \approx 0.5$ mM) suggests that specific binding would be difficult to differentiate from nonspecific background binding.

The slowed activation of WT HCN2 and HCN2_{ntk} channels induced by NFA can be largely accounted for by the negative shift in the voltage dependence of channel activation. However, for some mutant channels (i.e., R297Q, R294Q, or K291E channels; Fig. 6), NFA shifted the voltage dependence

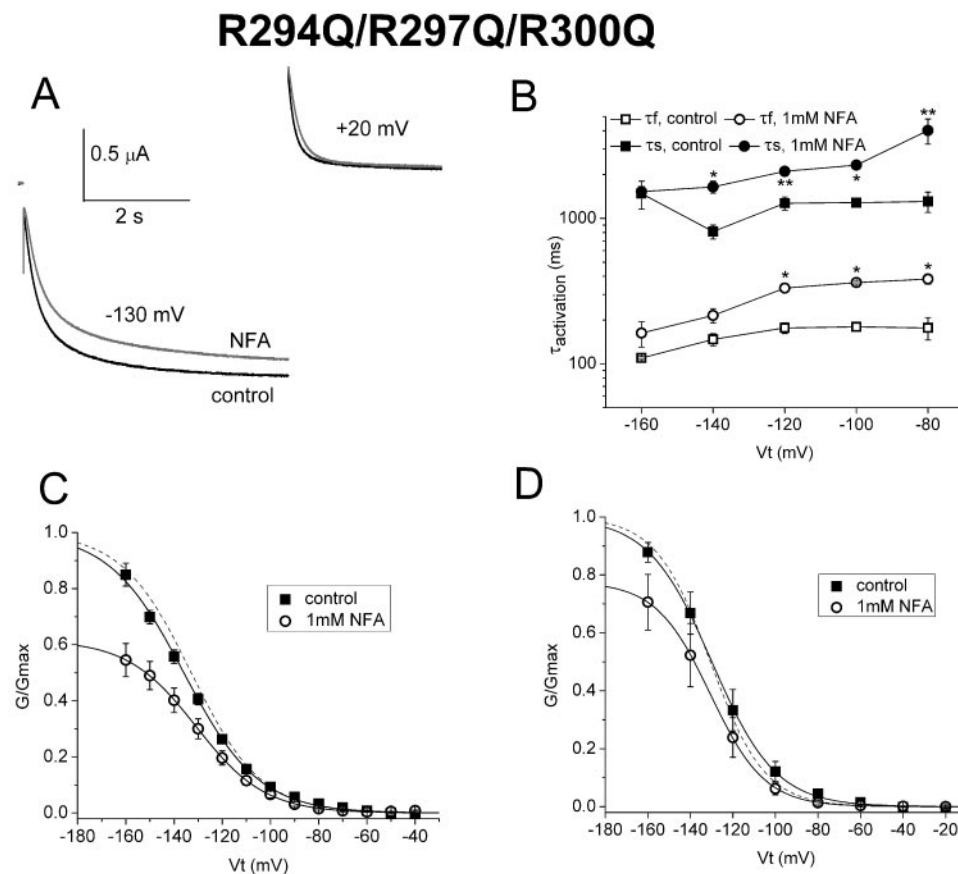


Fig. 9. Neutralization of Arg294, Arg297, and Arg300 residues in S4 domain prevents NFA-induced negative shift in the voltage dependence of activation of HCN2_{ntk} channels. **A**, triple mutant (R294Q/R297Q/R300Q) channel currents recorded from an oocyte during 5-s activating pulse to -130 mV, followed by pulse to +20 mV to record channel deactivation. For control: $\tau_f = 179$ ms, $\tau_s = 1056$ ms; $A_f/(A_f + A_s) = 0.70$. $\tau_{deact} = 167$ ms. For 1 mM NFA: $\tau_f = 188$ ms, $\tau_s = 1332$ ms; $A_f/(A_f + A_s) = 0.71$. $\tau_{deact} = 189$ ms. **B**, effect of 1 mM NFA on the kinetics of activation. Plotted data represent the average fast (open symbols) and slow (filled symbols) time constants for the onset of current activation during 5-s pulses at the indicated V_t . *, $p < 0.01$; **, $p < 0.05$ compared with matched control. **C** and **D**, normalized G-V relationships recorded before and after treatment of oocytes to 1 mM NFA. The test pulse durations used to elicit current were either 1 s (C) or 5 s (D). Smooth curves represent Boltzmann fit to the data. The dotted curves represent NFA data normalized to its own peak value.

of gating with no apparent effect or only a limited shift in the kinetics of activation. Some of this discrepancy might be due to the multiple activities of NFA in oocytes. NFA blocks an endogenous, hyperpolarization-activated Ca^{2+} -activated Cl^- channels in oocytes (White and Aylwin, 1990). Because the expression level of these channels varies considerably from one batch of oocytes to the next, the altered kinetics of HCN2 may result in part from block of endogenous Cl^- channels rather than a direct effect on HCN2 channel gating.

Blockers of cardiac pacemaker channels have been sought for treatment of disorders where a decrease in heart rate would be beneficial. For example, slower heart rates can help alleviate symptoms in angina pectoris or other forms of myocardial ischemia by reducing the metabolic requirement of cardiac muscle. I_f blockers such as ivabradine have been proposed for treating angina pectoris (Monnet et al., 2001; Vilaine, 2006) and may offer certain advantages over existing therapies. For example, both propranolol and ivabradine reduce exercise-induced ST segment shift in ischemia, but ivabradine preserved systolic shortening to a significantly greater degree than propranolol (Vilaine et al., 2003). Three I_f blocking drugs have been well characterized in native myocytes, and all exhibit kinetics consistent with gating-dependent interaction of drug with their receptor site. UL-FS49, ZD7288, and ivabradine decrease i_f in a voltage- and use-dependent manner consistent with preferential open-state channel block and access a binding site from the cytosolic side of the membrane (Bucchi et al., 2002). For all three drugs, channels must open before block can occur, and membrane hyperpolarization favors unblocking. Trapping of drug inside the channel by closure of the activation gate has been demonstrated for ZD7288 (Shin et al., 2001). NFA and related compounds represent a different mechanistic approach toward reduction of i_f in the heart. NFA reduces i_f magnitude primarily by a shift in gating with only a minor reduction due to a reduction in maximal conductance, presumed to result from direct block. In native cells, 0.1 mM NFA was reported to have no effect on the maximal conductance of i_f or i_h . At a 10 times higher concentration, we found that NFA reduced maximal conductance of HCN2 channels by 20 to 40%. It is unknown whether a drug that modifies HCN channel gating would confer any therapeutic advantage over a pore blocker.

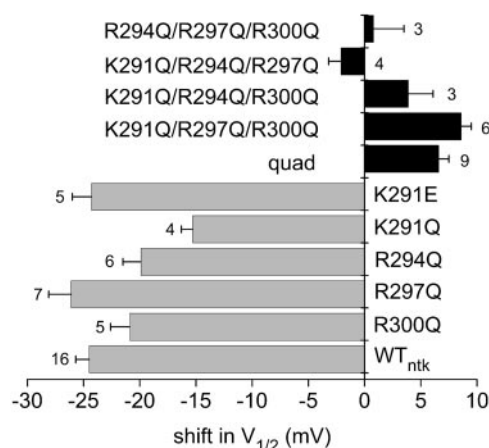


Fig. 10. Summary of NFA-induced shifts in $V_{1/2}$ for activation of HCN_{ntk} channel current. Voltage dependence of activation was determined using 5-s activating pulses before and after treatment of oocytes with 1 mM NFA. Number of oocytes is indicated at the end of each bar.

However, the effects of a gating modifier could be self-limiting. At high concentrations, a pore blocker can completely abolish channel current, whereas the maximal effect of a gating modifier would be limited to that caused by its maximum shift in activation (e.g., -38 mV for NFA). Discovery of a gating modifier that is more potent and channel-specific than NFA will be required before a meaningful comparison between the beneficial effects of a gating modifier and a pore blocker can be tested experimentally in animal models of myocardial ischemia.

Acknowledgments

We gratefully acknowledge the technical assistance of Kam Hoe Ng.

References

- Accili EA and DiFrancesco D (1996) Inhibition of the hyperpolarization-activated current (i_p) of rabbit SA node myocytes by niflumic acid. *Pflügers Arch* **431**:757–762.
- Bell DC, Yao H, Saenger RC, Riley JH, and Siegelbaum SA (2004) Changes in local S4 environment provide a voltage-sensing mechanism for mammalian hyperpolarization-activated HCN channels. *J Gen Physiol* **123**:5–19.
- Bucchi A, Baruscotti M, and DiFrancesco D (2002) Current-dependent block of rabbit sino-atrial node I_f channels by ivabradine. *J Gen Physiol* **120**:1–13.
- Busch AE, Herzer T, Wagner CA, Schmidt F, Raber G, Waldegger S, and Lang F (1994) Positive regulation by chloride channel blockers of IsK channels expressed in *Xenopus* oocytes. *Mol Pharmacol* **46**:750–753.
- Chen J, Mitcheson JS, Tristani-Firouzi M, Lin M, and Sanguinetti MC (2001) The S4–S5 linker couples voltage sensing and activation of pacemaker channels. *Proc Natl Acad Sci U S A* **98**:11277–11282.
- Chen J, Mitcheson JS, Lin M, and Sanguinetti MC (2000) Functional roles of charged residues in the putative voltage sensor of the HCN2 pacemaker channel. *J Biol Chem* **275**:36465–36471.
- Eskandari S, Zampighi GA, Leung DW, Wright EM, and Loo DD (2002) Inhibition of gap junction hemichannels by chloride channel blockers. *J Membr Biol* **185**:93–102.
- Goldin AL (1991) Expression of ion channels by injection of mRNA into *Xenopus* oocytes. *Methods Cell Biol* **36**:487–509.
- Jabeen T, Singh N, Singh RK, Sharma S, Somvanshi RK, Dey S, and Singh TP (2005) Non-steroidal anti-inflammatory drugs as potent inhibitors of phospholipase A2: structure of the complex of phospholipase A2 with niflumic acid at 2.5 Å resolution. *Acta Crystallogr D Biol Crystallogr* **61**:1579–1586.
- Lee YT and Wang Q (1999) Inhibition of hKv2.1, a major human neuronal voltage-gated K^+ channel, by meclofenamic acid. *Eur J Pharmacol* **378**:349–356.
- Liantonio A, Piccolo A, Babini E, Carbonara G, Fracchiolla G, Loidice F, Tortorella V, Pusch M, and Camerino DC (2006) Activation and inhibition of kidney CLC-K chloride channels by fenamates. *Mol Pharmacol* **69**:165–173.
- Liantonio A, Piccolo A, Carbonara G, Fracchiolla G, Tortorella P, Loidice F, Laghezza A, Babini E, Zifarelli G, Pusch M, et al. (2008) Molecular switch for CLC-K Cl^- channel block/activation: optimal pharmacophoric requirements towards high-affinity ligands. *Proc Natl Acad Sci U S A* **105**:1369–1373.
- Malykhina AP, Shoen F, and Akbarali HI (2002) Fenamate-induced enhancement of heterologously expressed HERG currents in *Xenopus* oocytes. *Eur J Pharmacol* **452**:269–277.
- Männikkö R, Elinder F, and Larsson HP (2002) Voltage-sensing mechanism is conserved among ion channels gated by opposite voltages. *Nature* **419**:837–841.
- Monnet X, Ghaleb B, Colin P, de Curzon OP, Giudicelli JF, and Berdeaux A (2001) Effects of heart rate reduction with ivabradine on exercise-induced myocardial ischemia and stunning. *J Pharmacol Exp Ther* **299**:1133–1139.
- Ottolia M and Toro L (1994) Potentiation of large conductance K_{Ca} channels by niflumic, flufenamic, and mefenamic acids. *Biophys J* **67**:2272–2279.
- Peretz A, Degani N, Nachman R, Uziyel Y, Gabor G, Shabat D, and Attali B (2005) Meclofenamic acid and diclofenac, novel templates of KCNQ2/Q3 potassium channel openers, depress cortical neuron activity, and exhibit anticonvulsant properties. *Mol Pharmacol* **67**:1053–1066.
- Piccolo A, Liantonio A, Babini E, Camerino DC, and Pusch M (2007) Mechanism of interaction of niflumic acid with heterologously expressed kidney CLC-K chloride channels. *J Membr Biol* **216**:73–82.
- Satoh TO and Yamada M (2001) Niflumic acid reduces the hyperpolarization-activated current (I_h) in rod photoreceptor cells. *Neurosci Res* **40**:375–381.
- Scott-Ward TS, Li H, Schmidt A, Cai Z, and Sheppard DN (2004) Direct block of the cystic fibrosis transmembrane conductance regulator Cl^- channel by niflumic acid. *Mol Membr Biol* **21**:27–38.
- Sesti F, Rajan S, Gonzalez-Coloso R, Nikolaeva N, and Goldstein SA (2003) Hyperpolarization moves S4 sensors inward to open MVP, a methanococcal voltage-gated potassium channel. *Nat Neurosci* **6**:353–361.
- Shin KS, Rothberg BS, and Yellen G (2001) Blocker state dependence and trapping in hyperpolarization-activated cation channels: evidence for an intracellular activation gate. *J Gen Physiol* **117**:91–101.
- Sinkkonen ST, Mansikkamäki S, Möykkynen T, Luddens H, Uusi-Oukari M, and Korpi ER (2003) Receptor subtype-dependent positive and negative modulation of GABA(A) receptor function by niflumic acid, a nonsteroidal anti-inflammatory drug. *Mol Pharmacol* **64**:753–763.

- Stühmer W (1992) Electrophysiological recording from *Xenopus* oocytes. *Methods Enzymol* **207**:319–339.
- Vaca L, Stieber J, Zong X, Ludwig A, Hofmann F, and Biel M (2000) Mutations in the S4 domain of a pacemaker channel alter its voltage dependence. *FEBS Lett* **479**:35–40.
- Vemana S, Pandey S, and Larsson HP (2004) S4 movement in a mammalian HCN channel. *J Gen Physiol* **123**:21–32.
- Vilaine JP (2006) The discovery of the selective I_f current inhibitor ivabradine A new therapeutic approach to ischemic heart disease. *Pharmacol Res* **53**:424–434.
- Vilaine JP, Bidouard JP, Lesage L, Reure H, and Pégliion JL (2003) Anti-ischemic effects of ivabradine, a selective heart rate-reducing agent, in exercise-induced myocardial ischemia in pigs. *J Cardiovasc Pharmacol* **42**:688–696.

- Wang HS, Dixon JE, and McKinnon D (1997) Unexpected and differential effects of Cl^- channel blockers on the Kv4.3 and Kv4.2 K^+ channels. Implications for the study of the I_{to2} current. *Circ Res* **81**:711–718.
- White MM and Aylwin M (1990) Niflumic and flufenamic acids are potent reversible blockers of Ca^{2+} -activated Cl^- channels in *Xenopus* oocytes. *Mol Pharmacol* **37**:720–724.

Address correspondence to: Michael C. Sanguinetti, Nora Eccles Harrison Cardiovascular Research and Training Institute, Department of Physiology, University of Utah, 95 South 2000 East, Salt Lake City, UT 84112. E-mail: sanguinetti@cvti.utah.edu
